Theor Appl Climatol (2012) 108:601–611
DOI 10.1007/s00704-011-0551-4

ORIGINAL PAPER

The heterogeneity of Meiyu rainfall over Yangtze–Huaihe River valley and its relationship with oceanic surface heating and intraseasonal variability

Dan-Qing Huang · Yong-Fu Qian · Jian Zhu

Received: 4 July 2011 / Accepted: 4 November 2011 / Published online: 30 November 2011
© Springer-Verlag 2011

Abstract Increasing heavy concentrated Meiyu precipitation over the Yangtze–Huaihe river valley (YHRV) during recent years has been previously reported. In fact, the concentrated Meiyu rainfall occurring in a small region or a certain period easily results in floods, thus it is worthy to analyze the heterogeneity of Meiyu rainfall over YHRV. In this study, we use both of precipitation concentration period (PCP) and precipitation concentration degree (PCD) based on vector analysis to identify the heterogeneity of Meiyu rainfall over YHRV. On the climatological mean, the concentrated heavy precipitation occurs in late summer over the Yangtze River Delta, where is usually suffered by floods. The dominant two patterns of PCP and PCD variations are northeast–southwest dipole pattern, homogeneous anomalies and homogeneous variation, north–south dipole pattern, respectively. In addition, the relationship on heterogeneity of Meiyu rainfall with sea surface temperature (SST) and the low level summer intraseasonal oscillation (ISO) are investigated. Two key regions of SST activities are found: Bay of Bengal (BOB) and Equatorial eastern Pacific. From BOB, more abundant water vapor has been brought. On the El Niño-Southern Oscillation variation, it is closely relative with PCD–PC1 during the decaying phase of El Niño, while PCP–PC2 is accompanied with developing phase of La Nina events, suggesting a negative feedback of PCP–PC2 on the Niño3.4 SST, and changes to positive during the later winter. On the ISO activities, the robust regions are located over the high-latitude areas, which are closely related with northeastern cold vortex. The north "cold and dry" air southwardly invaded with the lower-level strong warm air in the rainy area, and easily formed an "upper-wet and lower-dry" unstable layer. Under the trigger of the upward motion, the concentrated heavy rainfall easily occurred over YHRV. In all, the homogeneity variation of the concentrated heavy precipitation over YHRV is closely associated with both of the heating forcing (SST) and dynamical atmospheric forcing (low-level ISO).

D.-Q. Huang (✉) · Y.-F. Qian
School of Atmospheric Sciences, Nanjing University,
Nanjing 210093, China
e-mail: huangdq@nju.edu.cn

D.-Q. Huang
Key Laboratory of Meteorological Disaster of Ministry of Education,
Nanjing University of Information Science and Technology,
Nanjing, China

J. Zhu
State Key Laboratory of Hydrology-Water Resources and
Hydraulic Engineering, College of Hydrology and Water
Resources, Hohai University,
Nanjing 210098, China

1 Introduction

Monsoon is defined as a seasonal reversal of the prevailing wind that lasts for several months. Since the direction of this prevailing wind is associated with the precipitation amount, the rainfall has been used to study summer monsoons by many scientists (Chen et al. 2004; Wang and LinHo 2002; Wang et al. 2008). Weather and climate in the East Asia are mainly affected by the monsoon. Especially, the summer rainfall accounts for about 70% of the annual precipitation in this region, which is essential for the industry as a water resource in the East Asia. A notable example for severity and duration of rainfall is called Meiyu in China, Baiu in Japan, and Changma in Korea (hereafter referred to as the Meiyu). This rainy concentration is in a nearly east–west-elongated rainbelt during June and July, which stretches for many thousands of kilometers,

affecting China, Japan, Korea, and surrounding seas. During Meiyu season, the Yangtze–Huai River valley (YHRV, 110° E–122° E, 28° N–34° N) is vulnerable to floods and droughts, due to the relative concentration and severity of the rainfall amount (Tao and Chen 1987; Lau et al. 1988; Ding 1992). Therefore, it is worthy to understand the variations of Meiyu over YHRV.

Recently, concentrated heavy precipitation (CHP) has significantly increased over YHRV (Xu et al. 2009; Wang and Zhou 2005; Jiang et al. 2008; Huang et al. 2010). Scientists have paid more attention to CHP, as it caused significant economic loss. A decreasing trend in annual mean precipitation and extreme rain events was found in a zone extending from the southern part of Northeast China southwestward to the upper Yangtze River valley (Zhai et al. 2005). Zhang and Qian (2004) revealed the time when the CHP processes appeared in the middle and lower reaches of Yangtze River was different. In fact, the CHP indicates a heterogeneous pattern in spatial and temporal scale. Clearly, if during a certain period, the CHP occurs in one region, it is likely to result in disaster. Taking YHRV as example, since the distribution of annual precipitation is heterogeneity, the flood over YHRV mainly caused by extreme precipitation, especially in July. Floods are particularly dramatic if superposition of flood waves occurs (e.g., the floods in 1954 and 1998), when high waves from the Dongting (28.3° N–30.2° N, 110.4° E–113.1° E) and Poyang lake (28° N–29.5° N,115° E–116° E) basins meet with a flood wave on the mainstream Yangtze, and when the flood peaks from the upper and the middle/lower reaches coincide, which will cause a gigantic flood wave crest downstream. In the opposite, if time CHP occurred are inconsistent along Yangtze–Huaihe River, the floods can be staggered. Thus, understanding the features and physical processes for heterogeneity of Meiyu rainfall over YHRV is very important.

The Meiyu is also one of the key links among circulation variations over the mid-latitude North Pacific. According to the climate dynamics, the mid-latitude climate variations are closely related to two types of forcing: the external atmospheric forcing such as sea surface temperature (SST) anomalies and the internal dynamic processes operating with the atmosphere itself such as the synoptic-scale transient eddy or intraseasonal oscillation (ISO; Ren and Zhang 2007). The variability of Meiyu rainfall over eastern China is strongly modulated by the East Asian monsoon, which is related to the tropical SST, like Western Pacific Warm Pool (Huang and Sun 1992), El Niño-Southern Oscillation (ENSO, Wang et al. 2000; Li et al. 2010), and Indian Ocean (Annamalai et al. 2005).

Besides SST, the boreal summer ISO has strong impacts on the onset, withdrawal, and intraseasonal variability (e.g., active and break phases) of Meiyu systems over YHRV (Lau and Chan 1986; Annamalai and Slingo 2001; Seo et al. 2007), especially on the low-level ISO patterns at 850 hPa (Yang and Li 2003; Yang 2009; Goswami et al. 2006; Jiang et al. 2004; Teng and Wang 2003). These investigations depict close relationships between the external atmospheric forcing anomalies, the internal dynamic processes and variations of Meiyu systems.

As an important element in Asian summer monsoons, the year-to-year variation of the heterogeneity of Meiyu over YHRV is necessarily linked with the oceanic heating anomaly. Meanwhile, the synoptic-scale transient eddy also shows a critical role in Asian summer monsoon variations. Based on these considerations, our aims are to answer the following questions:

1. What are the major modes of the heterogeneity of Meiyu over YHRV?
2. What are the links between the heterogeneity anomalies of Meiyu over YHRV, SST and low-level ISO activities?

The paper is organized as follows. The data used are described in Section 2. Section 3 provides a brief description of the methodology for identifying the heterogeneity of Meiyu rainfall. The results are discussed in Section 4, including the climatology, the anomalies variations, and their relationship with SST and low-level ISO. The conclusions are provided in Section 5.

2 Data

The observations of China daily precipitation data at 422 stations over YHRV (Fig. 1) from the National Meteorological Information Center during the period of 1960–2007 are used in this study. This data was provided by the National Meteorological Information Center, China Meteorological Administration. In this study, since the Meiyu period can be defined as June and July, daily precipitation data in June and July is chosen.

SST data from the Global Sea Surface Temperature dataset for the period 1960–2007 with a spatial resolution of 1°(latitude)×1°(longitude) provided by British Meteorological Office is used to represent the heat transfer between air and ocean (Rayner et al. 2003).

The atmospheric dataset for the analysis is from National Centers for Environmental Prediction–National Center for Atmospheric Research (NCEP/NCAR) reanalysis daily dataset for the period 1960–2007 (Kalnay et al. 1996). The variables are on 2.5° (latitude)×2.5° (longitude) grids. In this study, the variables used are meridional and zonal winds at 850 hPa for calculating the low-level ISO winds which represent the dynamical effects.

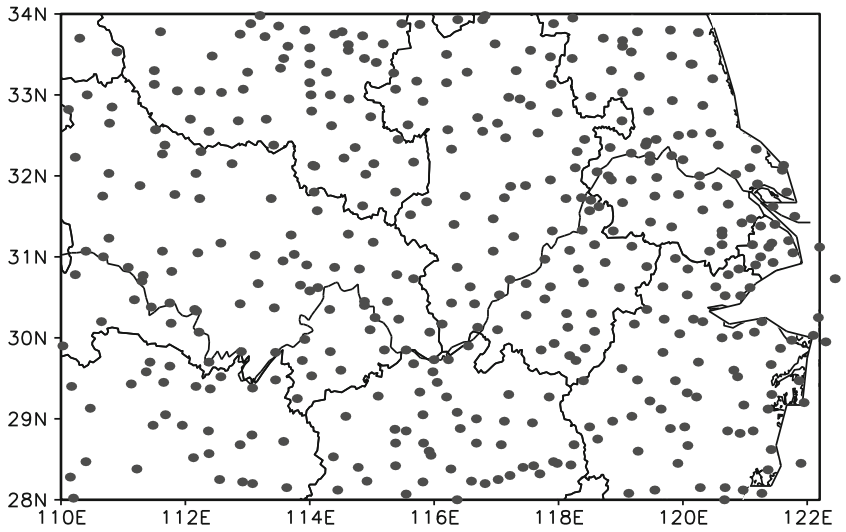

Fig. 1 The station distribution of dataset used in this study

According to the band-pass-filtered technique based on Murakami (1979), the ISO fluctuations associated with disturbances with a 30–60-day period have been extracted from the NCEP/NCAR daily dataset.

The statistic techniques of empirical orthogonal function (EOF) analysis, linear regression, and correlation are used in this study. The significance of correlation and linear regression is assessed by *t* test.

3 Methodology

In this study, based on the precipitation concentration period (PCP) and precipitation concentration degree (PCD) defined by Zhang and Qian (2003, 2004) and Zhu et al. (2010), the following equations are used to calculate PCP and PCD for identifying the heterogeneity of Meiyu rainfall over YHRV.

$$\begin{cases} \mathrm{PCP}_i = \arctan\left(R_{xi}/R_{yi}\right) & (1) \\ \mathrm{PCD}_i = \sqrt{R_{xi}^2 + R_{yi}^2}/R_i & (2) \end{cases} \quad R_i \neq 0$$

where, $R_{xi} = \sum_{j=1}^{N} r_{ij} \times \sin\theta_j$; $R_{yi} = \sum_{j=1}^{N} r_{ij} \times \cos\theta_j$; $\theta_j = \frac{360^\circ}{61} \times j$ (i=1, 2, 3,…, 48, is the year number, j=1,2,3,…, 61, is the jth day in summer). R_i denotes the total Meiyu precipitation in ith year. The two indices are dimensionless. The basic principle for calculating the PCP and PCD is vector analysis, considering the daily precipitation vector (R_{xi}, R_{yi}). Clearly, it is well known that June and July are the dominant rainy season over YHRV, thus the R_i is exactly above 0. We can ignore the conditions when R_i=0. The closer of PCD value to 1, the more CHPs occurred over YHRV. Based on the definition, each station has a pair of PCP and PCD for identifying the heterogeneity of Meiyu rainfall in each year.

The Meiyu period (June–July) contains 61 days, which have been projected in a circle (360°). θ_j indicates the vector angle for jth day during Meiyu period (Fig. 2). We take the June 1st and July 31st as examples for calculating θ_j. June 1st is the first day during Meiyu period, and θ_1 is defined as $\frac{360^\circ}{61} \times 1 = 5.9^\circ$ (Fig. 2). July 31st is the 61st day during Meiyu period and θ_{61} is defined as $\frac{360^\circ}{61} \times 61 = 360^\circ$.

The physical interpretations of PCP and PCD reflect the heterogeneity distribution of Meiyu rainfall over YHRV. During Meiyu period, if the precipitation occurs just in 1 day, PCP is that day and PCD is 1, the largest value; if the daily precipitation is same in each day during the whole Meiyu period, the PCP is the middle day of Meiyu period and PCD is 0. The large (small) value of PCD indicates the heavy precipitation events concentrates (disperse) during Meiyu period. The PCP indicates the time when heaviest

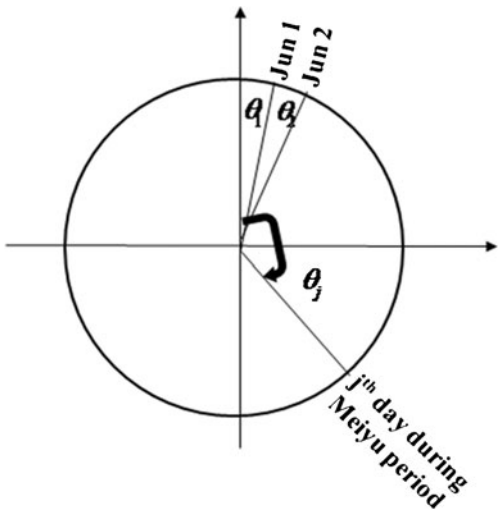

Fig. 2 The distribution of the angle range (θ_j) of each day during Meiyu period

precipitation occurs. The large (small) value indicates the CHP events occur later (earlier). PCP and PCD are not isolated concepts. Combining PCP and PCD can well describe the heterogeneity of precipitation events. For example, the PCP and PCD of station A and B are 13, 0.9, and 32, 0.2, respectively. That suggests the CHP events in station A and B is likely to occur around June 13 and July 2, respectively. Comparing the PCD of station A and B, the heavy precipitation is more concentrated in station A than in station B.

4 Results and discussions

4.1 The daily evolution of Meiyu rainfall over YHRV in 1978 and 1998

Based on the daily precipitation data of 422 stations over YHRV, the daily evolution and standard deviations of Meiyu rainfall in 1978 and 1998, which are taken as the example of non-CHP and CHP, respectively, are given in Fig. 3.

In 1978, several precipitation peaks are found in Fig. 3a. Combined with the standard deviation, largest centers appear in northern and southeastern part of YHRV (Fig. 3c). The averaged standard deviation over YHRV is about 10.4. In 1998, the heavy precipitation concentrates around in the middle of Meiyu period (nearly from June 11 to 26, Fig. 3b), when is accordance with the time disastrous flood occurred (Wang et al. 2003; Xu and Zhang 2007). On the standard deviation (Fig. 3d), the maximum center locates over the middle of YHRV and the values are around 30. Both considering the changes of the daily evolution and standard deviation in 1978 and 1998, the day-to-day variation of Meiyu precipitation is larger in 1998 than in 1978. Based on the two examples, the heterogeneity of Meiyu rainfall can be found over YHRV.

4.2 The climatology of summer PCP and PCD over YHRV

The climatology of summer PCP and PCD over YHRV during the period of 1960–2007 are given in Fig. 4. The maximum PCP center (around 40, July 10) is located over Yangtze River Delta (YRD, 28° N~32° N, 119° E~122° E), and the minimal center (about 34, July 4) is found near the southern part of YHRV, suggesting the concentrated heavy precipitation appeared later over YRD, and earlier in southern part of YHRV. On the PCD distribution (Fig. 4b), the maximum PCD is located near the coastal area. The present analysis indicated that CHP is mainly occurred nearly 39th or 40th day in summer (about July 9 or 10) over YRD. Indeed, this region is easier to be suffered by floods (Dong et al. 2009; Zhu et al. 2007; Wu et al. 2006; Su et al. 2008; Wang and Zhou 2005).

4.3 The summer PCP and PCD variability over YHRV

The EOF analysis is performed to summer PCP and PCD anomalies over YHRV during 1960–2007. The variances of the first two modes are 22%, 10% for PCP and 21%, 12%

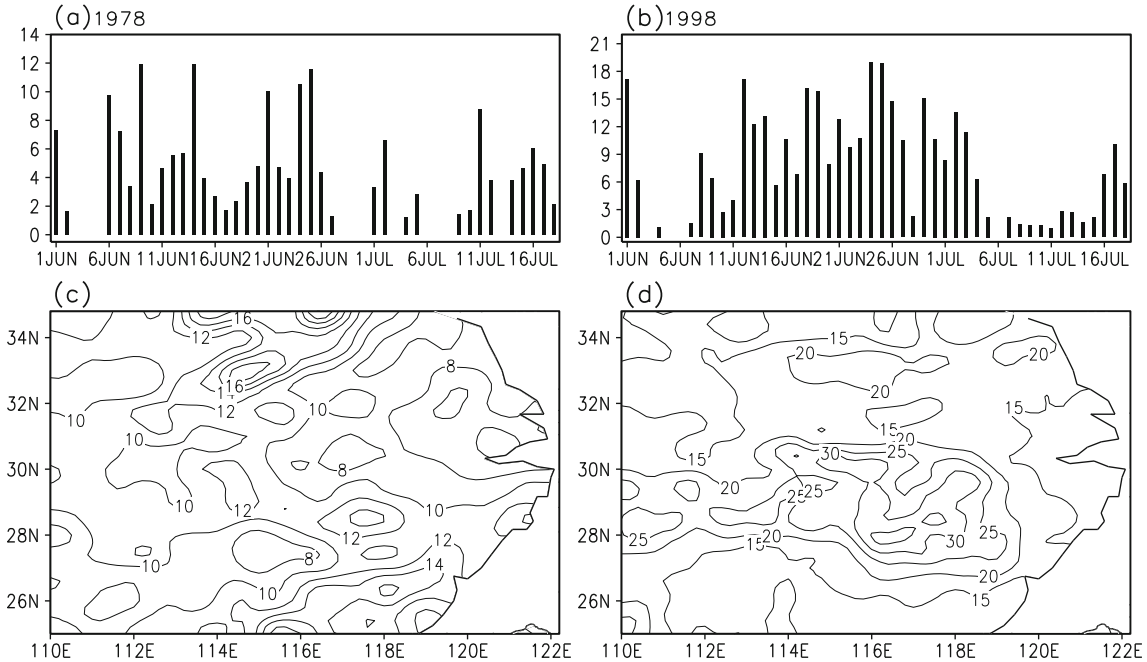

Fig. 3 The daily evolution of regional mean precipitation during Meiyu period (**a**, **b**) and the standard deviations of Meiyu rainfall over YHRV (**c**, **d**); **a**, **c** 1978; **b**, **d** 1998

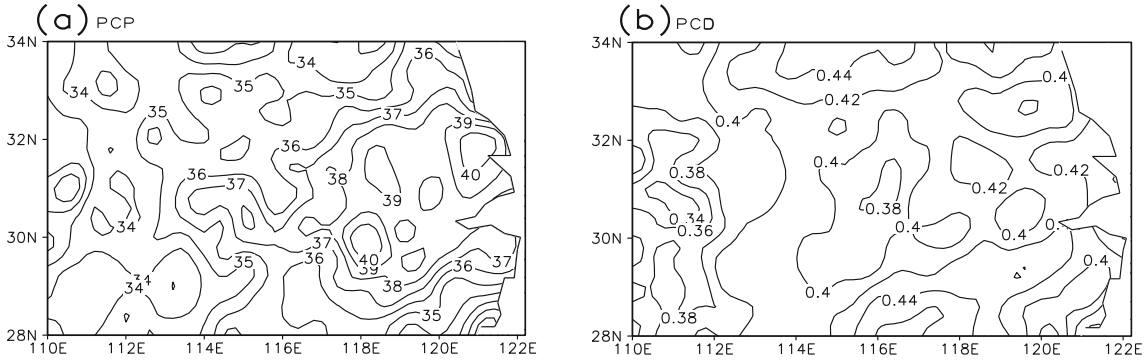

Fig. 4 The climatological distribution of PCP (**a**) and PCD (**b**) over YHRV during Meiyu period

for PCD, respectively. According to the rule given by North et al. (1982), these two leading modes of PCP and PCD are statistically distinguished from the rest of the eigenvectors in terms of the sampling error bars.

The spatial patterns of the first two EOF leading modes of PCP, and their corresponding time coefficients measured in units of their respective standard deviation (denoted as PCP–PC1 and PCP–PC2, respectively) are plotted in Fig. 5.

The dominant pattern (EOF1) characterized by a northeast–southwest dipole with earlier and later CHP occurred over YHRV (Fig. 5a). Combined with the PCP_PC1 (Fig. 5b), in the positive PCP_PC1 years, the concentrated precipitation occurred earlier over northeastern YHRV and later over southwestern YHRB. In the negative PCP_PC1 years, the results are vice verse. The second pattern of PCP (EOF2, Fig. 5c) is homogeneous PCP anomalies.

The spatial patterns of the first two EOF leading modes of PCD, and their corresponding time coefficients measured in units of their respective standard deviation (denoted as PCD–PC1 and PCD–PC2, respectively), are plotted in Fig. 6. The dominant feature of first pattern (EOF1) of PCD (Fig. 6a) is homogeneous PCD anomalies over the whole YHRV. As shown in Fig. 6b, in the positive PCD_PC1 years, CHP easily occurred over YHRV. In the negative PCD_PC1 years, the results are vice verse. The second pattern (Fig. 6c) indicates"+ −" variation spanning from northern to southern part of YHRV along the Yangtze River, suggesting out of phase changes along 30° N of YHRV.

In order to get the dominant periods of PC time series, the four PC time series have been departed into three types: linear trend, decadal, and interannual variations. The variances of each part have been given in Table 1. Clearly,

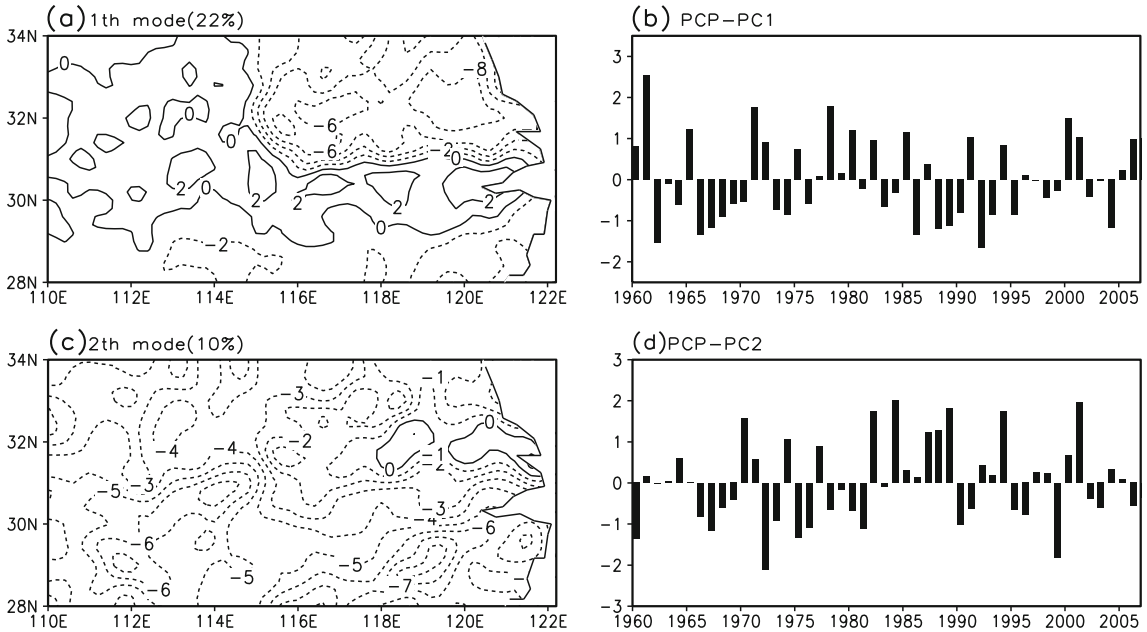

Fig. 5 The spatial patterns (**a**, **c**) and time coefficients (**b**, **d**) of the first two EOF leading modes of PCP over YHRV during 1960–2007. The time coefficients (*bars*) are measured in units of their respective standard deviation

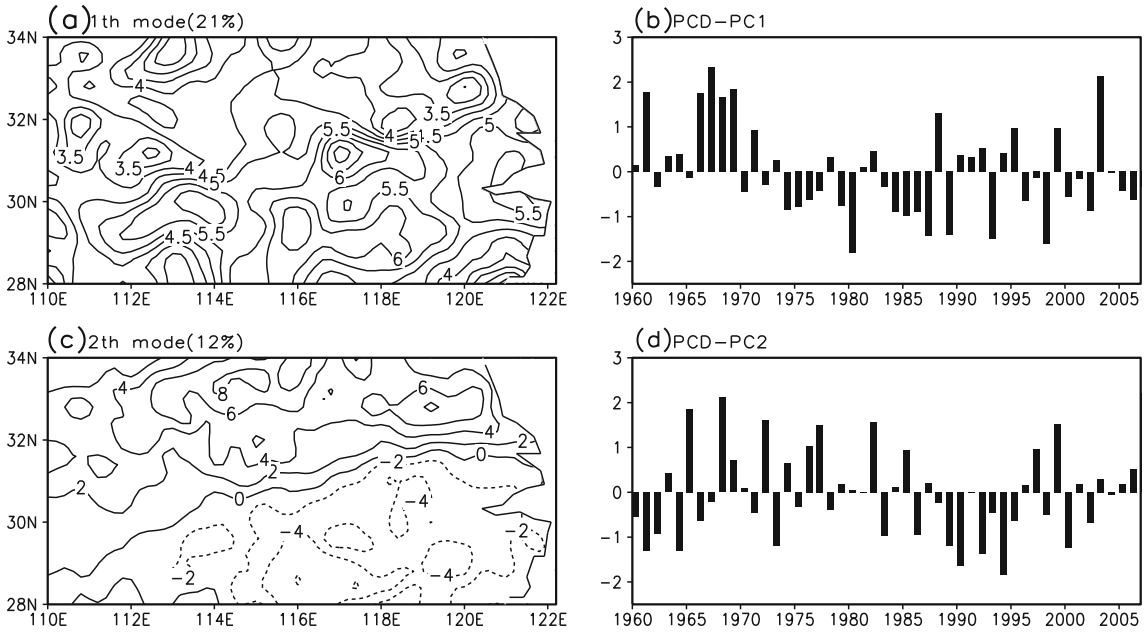

Fig. 6 Same as Fig. 5 except for PCD

the first two dominant time periods are the interannual and decadal variation. That suggests the four PC time series are mostly on decadal and interannual timescales.

4.4 Associations of summer PCP and PCD anomalies with SST and low-level ISO

Since the four PC time series mostly contain decadal and interannual variations. Firstly, we examine the relationship between the dominant EOF modes and summer monsoon on decadal scale. According to PCP–PC1 and PCD–PC1, the significant positive and negative cases were calculated by the criterion that the standard deviation anomaly should exceed ±1. The typical anomalous cases are listed in Table 2. In order to analyze the interdecadal changes between PCP–PC1, PCD–PC1 and summer monsoon, we have divided the significant cases into two groups: 1960–1979 and 1980–2007, since previous studies have suggested that East Asian climate has experienced an interdecadal scale transition since the late 1970s (Hu 1997; Zhou et al. 2009a, b; Yu et al. 2004; Yu and Zhou 2007).

Table 1 The variances of linear trend, inter-annual, decadal variation on PCP–PC1, PCP–PC2, PCD–PC1, and PCD–PC2 (units: %)

	Linear trend variation	Inter-annual variation	Decadal variation
PCP–PC1	7.4	67.2	25.4
PCP–PC2	13.6	55.8	30.6
PCD–PC1	0.5	72.1	27.4
PCD–PC2	18.5	56.4	25.1

The composition of low level winds and the moisture divergence have been given in Fig. 7. Apparently, the variations of low level winds in two periods are different. On the PCP–PC1 (Fig. 7a, c), southeastern wind anomalies with water vapor transport from Indian Ocean to YHRB during 1980–2007, while in 1960–1979, the water vapor is located over Bay of Bengal (BOB), and southeastern wind anomalies transport into northeastern China. These features are in accordance with the precipitation pattern in Asian summer monsoon systems (Zhou et al. 2009a, b). On the PCD–PC1 (Fig. 7b, d), the stronger southeastern wind anomalies transport from Indian Ocean to the northern part of China in 1960–1979, while during 1980–2007, northern wind anomalies are located over most eastern China. On the SST variations (figure omitted), significant negative anomalies have been found over the Equatorial eastern Pacific associated with ENSO, during 1980–2007. Thus, the dominant PCP and PCD time serial can be linked with the Asian summer monsoon on decadal variation.

Secondly, since the dominant variation of PCs is interannual variation, we perform a regression analysis using the PCs as a reference time series to examine how different EOF modes are related to the external atmospheric forcing and the internal dynamic processes on the interannual scale.

Figure 8 illustrates the patterns of regression of the summer SST and low-level ISO at 850 hPa, against the normalized PCP–PC1 and PCP–PC2, respectively. The significant regressed anomalies, corresponding to the SST against the normalized PCP–PC1 and PCP–PC2 (Fig. 8a, c), are found in two regions: northern Pacific, Equatorial eastern Pacific. In Fig. 8c, the homogeneous variation of PCP over

Table 2 Positive and negative years according to PCP–PC1 and PCD–PC1 during 1960–1979 and 1980–2007

	1960–1979	1980–2007
Positive PCP–PC1	1961, 1965, 1971, 1978	1985, 1991, 2000, 2001, 2006, 2007
Negative PCP–PC1	1962, 1966, 1967	1980, 1986, 1988, 1989, 1992, 2004
Positive PCD–PC1	1961, 1966, 1967, 1968, 1969	1988, 1999, 2003
Negative PCD–PC1		1980, 1987, 1989, 1993, 1998

YHRV is strongly related to ENSO events via the significant changes of the convention over the tropical region and consequently changed atmospheric circulations over the mid-low latitudes (Matthews and Kiladis 1999).

The patterns of regression of low level ISO against the normalized PCP–PC1 and PCP–PC2 are shown in Fig. 8b, d, respectively. Figure 8b indicates that the heavy precipitation occurs earlier/later in northeast/southwest over YHRV is accompanied by the significant cyclone and anticyclone ISO anomalies in the northeastern North Pacific extending from west to east. In Fig. 8d, significantly northwestward and southwestward ISO anomalies are extending from west to east at the high latitude. In all, both of the two PCs, the robust regions are located over high latitude, which is close related with northeastern cold vortex (NCV; He et al. 2007).

Similarly, Fig. 9 gives the patterns of regression of the summer SST and ISO at 850 hPa, against the normalized PCD–PC1 and PCD–PC2. In Fig. 9a, the significant decreasing anomalies of SST in Equatorial eastern Pacific are related with the homogeneous-variation over the whole YHRV area. The regressed SST anomalies (Fig. 9c) is concentrated in BOB, which is in accordance with the "− +"dipolar pattern of PCD. On the patterns of regression of ISO against the normalized PCD–PC1 and PCD–PC2, Fig. 9b shows that the homogeneous variation of PCD over YHRV is accompanied by the significant ISO anomalies which direct northeastward and southeastward scattering from BOB.

Analysis above revealed two significant key regions on the SST activities: Equatorial eastern Pacific and BOB. On the ISO anomalies, according to PCP–PC1 and PCP–PC2, the robust region locates over high latitude, which is associated with NCV.

To further examine these relationships, firstly, we use the SST averaged over BOB (10° N~20° N, 75° E~110° E) as an index of BOB and NCV index is defined by He et al. (2007; the contrary of the average temperature at 1,000 hPa in June–July in the area of 37° N~45° N, 127° E~145° E) and correlates them with the averaged PCP over YHRV

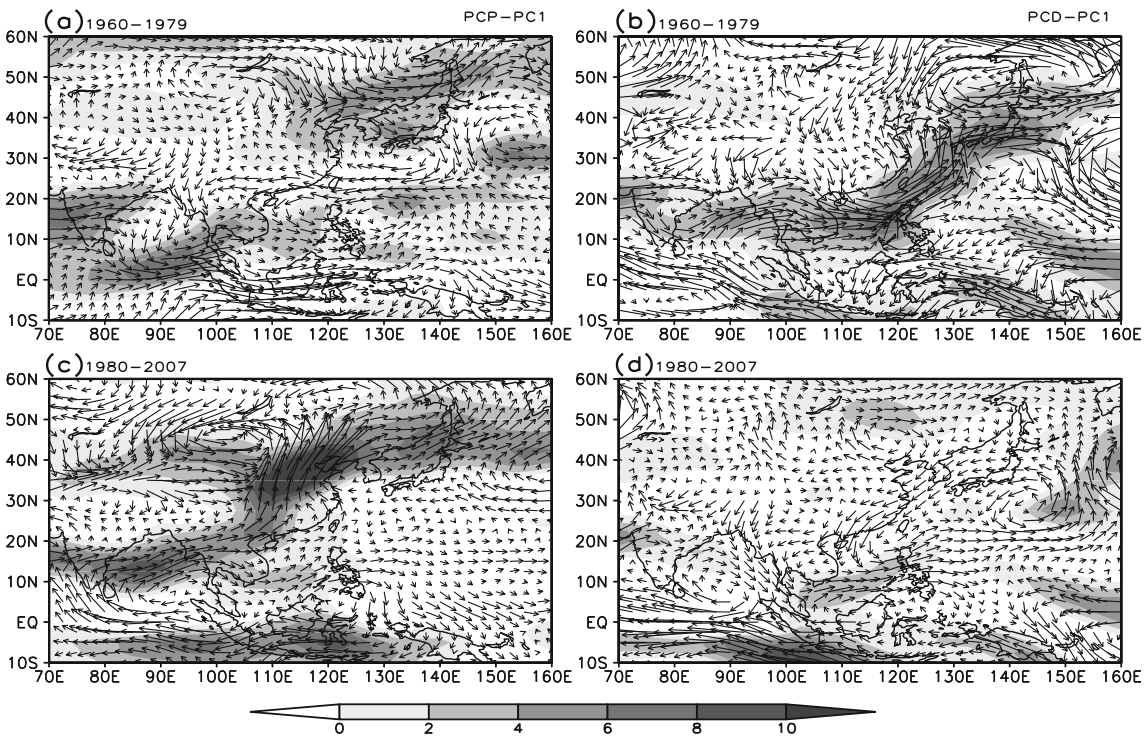

Fig. 7 Differences (positive case minus negative case of PCP–PC1 (**a**, **c**) and PCD–PC1(**b**, **d**)) of composition of low level winds at 850 hPa (unit: m/s) and moisture convergence (integration 1,000–300 hPa; unit, $10^3 \times gm^{-2}\ s^{-1}$) during 1960–1979 (**a**, **b**) and 1980–2007 (**c**, **d**)

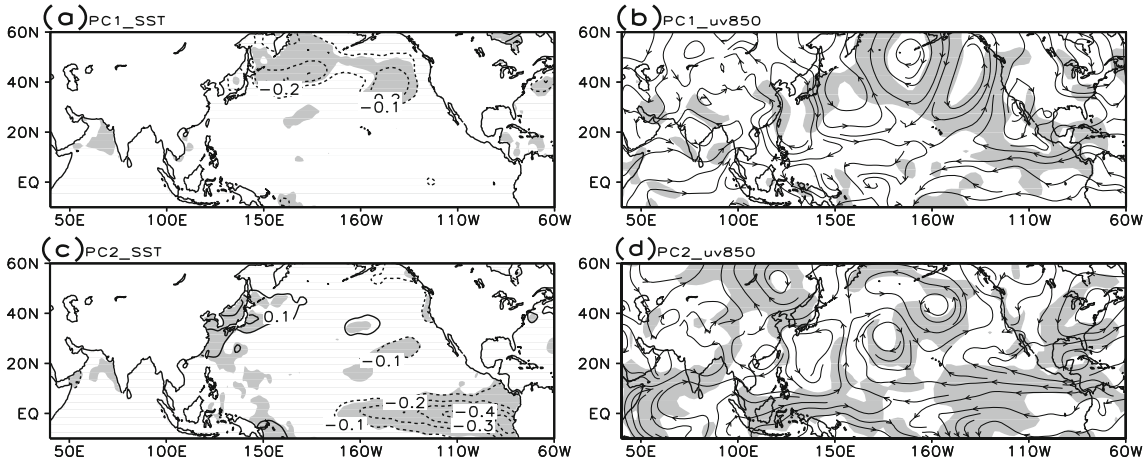

Fig. 8 SST (**a**, **c**) and the ISO wind anomalies at 850 hPa (**b**, **d**) regressed upon the PCP_PC1 and PCP_PC2, respectively. Values with magnitude larger than 90% confidence level are shaded

during 1960–2007. The correlation pattern shows great positive over the whole YHRV and a positive center in the middle of YHRV, respectively (Fig. 10). This strongly suggests a potential link between the PCP anomalies over YHRV and SBOB, NCV. These features are similar to those discovered recently (He et al. 2007). They indicate that the north "cold and dry" air southwardly invaded with the lower-level strong warm air in the rainy area, and easily formed an "upper-wet and lower-dry" unstable layer. Under the trigger of the upward motion, it will easily result in the significant increase of the concentrated precipitation over YHRV. Meanwhile, since SBOB is one of the most important water vapor sources providing the summer rainfall over YHRV (Jiang et al. 2009; Zhou et al. 2010), the SBOB will bring abundant water vapor to YHRV. Under the two conditions, the concentrated summer rainfall more easily occurs over YHRV.

Secondly, in order to find the relationship between PCP–PC2, PCD–PC1 and the different phase of ENSO events, we carried out a lead-lag correlation analysis between PCP–PC2, PCD–PC1 and monthly mean Niño3.4 index from January of the previous year to December of the later year. The Niño3.4 index is found at http://www.esrl.noaa.gov/psd/data/climateindices/list/. On the PCD–PC1 (Fig. 11), after the early summer in year (0), PCD–PC1 is significantly positively correlated with the Niño3.4 index, thus this PC is accompanied with decaying El Niño. Moreover, this positive correlation is till to winter in year (0) and later spring. From the summer of year (0) to later autumn of year (0), PCP–PC2 is significantly negatively correlated with the Niño3.4 index, thus PCP–PC2 is accompanied with developing phase of La Nina events, suggesting a negative feedback of PCP–PC2 on the Niño3.4 SST, and changes to positive during the later winter. In fact, previous studies have suggested that the tropical Pacific SST plays important roles in the variations of rainfall over eastern China (Chang et al. 2000a, b). ENSO can affect Asian summer monsoon directly via large-scale circulation changes,

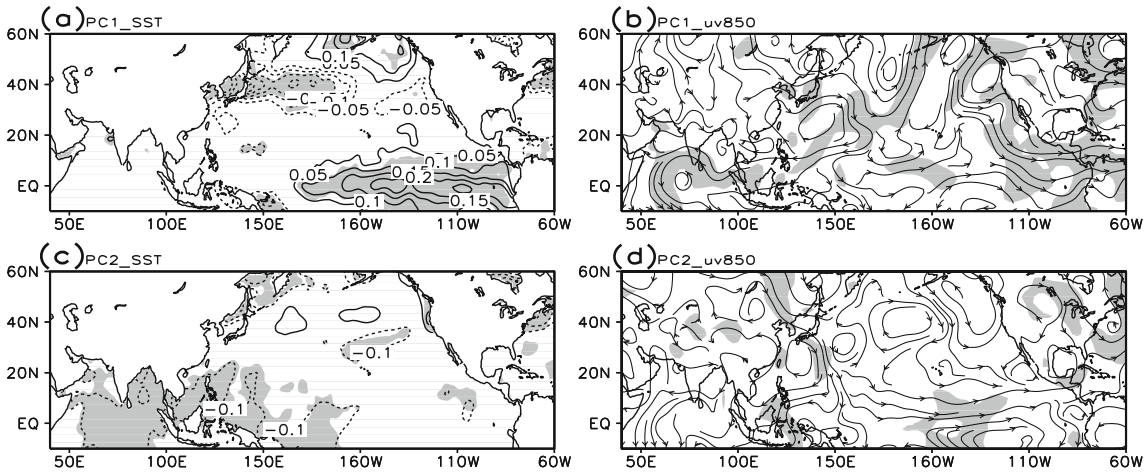

Fig. 9 Same as Fig. 8 except for PCD_PC1 and PCD_PC2

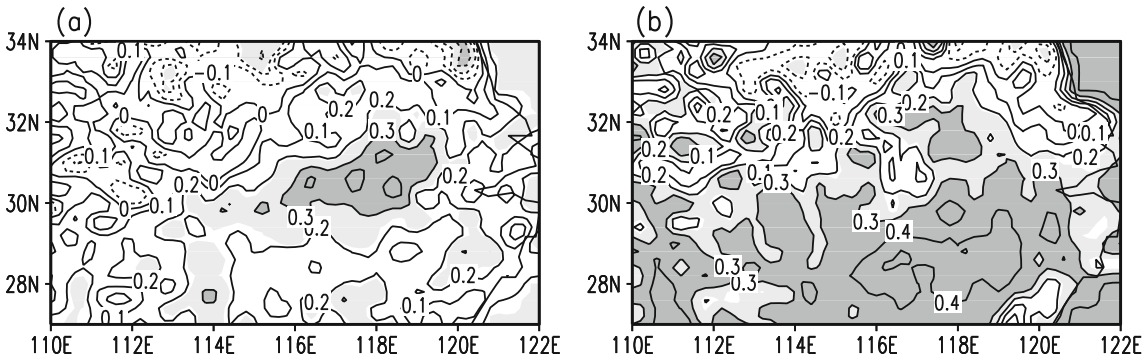

Fig. 10 The correlation between regional mean PCP and (**a**) index of BOB, (**b**) NCV index during 1960–2007

especially during different period of ENSO (Wu et al. 2009, 2010). The changed SST activities are found in Equatorial eastern Pacific, then the circulation over East Asia (e.g., western Pacific subtropical high) will change (Lau and Nath 2009; Zhang et al. 2007; Alexander et al. 2004), which will directly affect the Meiyu precipitation over YHRV, including the heterogeneity of Meiyu rainfall.

5 Conclusions

The present study examined the heterogeneity of Meiyu rainfall over YHRV and its coupled relationship with SST and low-level ISO activities. For this purpose, we imposed to identify the heterogeneity of Meiyu rainfall by the PCP and PCD based on vector analysis. Results suggest that the dominant and second patterns of PCP variation show northeast–southwest dipole variation and homogenous anomalies, respectively; PCD variations are characterized by homogenous anomalies and north–south dipole patterns, respectively. The corresponding four PC time series are mostly on decadal and interannual timescales.

On the decadal scale, both of PCP–PC1 and PCD–PC1 time serials can be linked with the Asian summer monsoon on decadal scale. On the interannual scale, the regressed analysis displays a coupled mode among the heterogeneity of Meiyu rainfall over YHRV, oceanic surface heating anomalies and ISO anomalies. Two key regions on SST activities are found: Equatorial eastern Pacific and BOB. On the ISO activities, the heterogeneity of Meiyu rainfall over YHRV is strongly related with the ISO activities located over the high-latitude regions and BOB.

The tropical Pacific and BOB SST play important roles in the variations of rainfall over eastern China, since abundant water vapor is brought from BOB. Meanwhile, the north "cold and dry" air southward and the lower-level strong warm air intersected in the rainy area and formed an "upper-wet and lower-dry" unstable layer. Under the trigger of the upward motion, it will easily result in the significant increase of the heavy precipitation over YHRV. On the SST anomalies over Equatorial eastern Pacific, the PCD–PC1 is significantly positively correlated with the Niño3.4 index, suggesting this PC is accompanied with decaying El Niño. The PCP–PC2 is accompanied with developing phase of La Nina events, suggesting a negative feedback of PCP–PC2 on the Niño3.4 SST, and changes to positive during the later winter. Therefore, the heterogeneity of CHP variation is closely associated with both of the heat forcing (SST) and dynamical atmospheric forcing (low-level ISO).

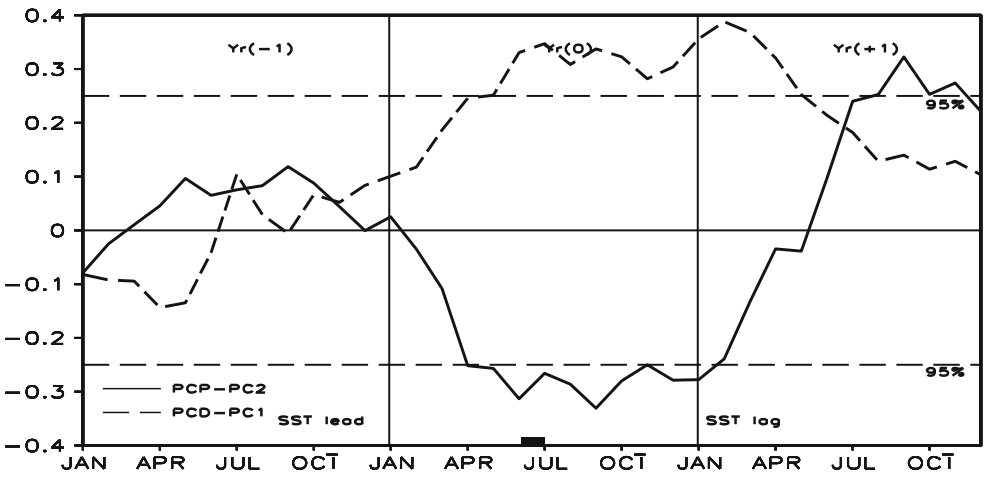

Fig. 11 The lead–lag correlation coefficients between PCP–PC2 (*solid curve*), PCD–PC1(*dashed curve*) and monthly mean Niño3.4 SST index from January of the preceding year (Yr(−1)) to December of the later year (Yr(+1)). The *dashed gray lines* denote the 5% significant level. The *black bar* indicates the simultaneous period (June and July) in the reference year (Yr(0))

In this study, only SST in North Pacific is demonstrated as the presentation of the external forcing. However, the relationship between other persistent external forcing (e.g., latent heating and sensitive heating) should be investigated comprehensively. Moreover, the related numerical simulation and dynamical analysis should be carried out in future work.

Acknowledgments We thank the editor and three anonymous reviewers for their valuable comments and suggestions. The NCEP/NCAR reanalysis data was provided by the National Centers for Environmental Prediction (NCEP) and National Center for Atmospheric Research (NCAR). This study is jointly sponsored by National Natural Science Foundation of China (Grant Nos. 41105044 and 41130963), the National Basic Research Program of China (973 Program; grant no. 2011CB952002), the Open Project Program of Key Laboratory of Meteorological Disaster of Ministry of Education (Nanjing University of Information Science and Technology; grant no. KLME1105), Fundamental Research Funds for the Central Universities (Grant no. 1107020730 and 1084020702), and the Research Fund for the Doctoral Program of Higher Education (grant no. 20100091110003).

References

Alexander MA, Lau NC, Scott JD (2004) Broadening the atmospheric bridge paradigm: ENSO teleconnections to the tropical West Pacific-Indian Oceans over the seasonal cycle and to the North Pacific in summer. Earth's climate: the ocean–atmosphere interaction. Geophys Monogr 147:85–103

Annamalai H, Slingo JM (2001) Active/break cycles: Diagnosis of the intraseasonal variability of the Asian Summer Monsoon. Clim Dyn 18:85–102

Annamalai H, Liu P, Xie SP (2005) Southwest Indian Ocean SST variability: its local effect and re-mote influence on Asian monsoons. J Clim 18:4150–4167

Chang CP, Zhang Y, Li T (2000a) Interannual and interdecadal variations of the East Asian summer monsoon and tropical Pacific SSTs. Part I: roles of the subtropical ridge. J Clim 13:4310–4325

Chang CP, Zhang Y, Li T (2000b) Interannual and interdecadal variations of the East Asian summer monsoon and tropical Pacific SSTs. Part II: meridional structure of the monsoon. J Clim 13:4326–4340

Chen TC, Wang SY, Huang WR et al (2004) Variation of the East Asian summer monsoon rainfall. J Clim 17:744–762

Ding YH (1992) Summer Monsoon rainfalls in China. J Meteorol Soc Jpn 70:373–396

Dong S, Ding YH, Liu YJ (2009) Decadal northward shift of the Meiyu belt and the possible cause. Chinese Sci Bull 54:4742–4748

Goswami BN, Wu G, Yasunari T (2006) The annual cycle, intraseasonal oscillations, and roadblock to seasonal predictability of the Asian summer monsoon. J Clim 19:5078–5099

He JH, Wu WZ, Jiang ZH et al (2007) "Climate effect" of the northeast cold vortex and its influences on Meiyu. Chinese Sci Bull 52:671–679

Hu ZZ (1997) Interdecadal variability of summer climate over East Asia and its associated with 500 hPa height and global sea surface temperature. J Geophys Res 102(D16):19403–19412

Huang RH, Sun FY (1992) Impacts of the tropical western Pacific on the East Asian summer monsoon. J Meteorol Soc Jpn 70 (1B):243–256

Huang DQ, Zhu J, Kuang XY (2010) Decadal variation of different durations of continuous Meiyu precipitation and the possible cause. Chinese Sci Bull 56:424–431

Jiang X, Li T, Wang B (2004) Structures and mechanisms of the northward propagating boreal summer intraseasonal oscillation. J Clim 17:1022–1039

Jiang T, Kundzewicz ZW, Su B (2008) Changes in monthly precipitation and flood hazard in the Yangtze River Basin. China. Int J Climatol 28:1471–1481

Jiang XW, Li YQ, Wang X (2009) Water vapor transport over China and its relationship with drought and flood in Yangtze River Basin. J Geogr Sci 19(2):153–163

Kalnay E, Kanamitsu M, Kistler R et al (1996) The NCEP/NCAR 40-year Reanalysis Project. Bull Am Meteorol Soc 77:437–472

Lau KM, Chan PH (1986) Aspects of the 40–50 day oscillation during the northern summer as inferred from the outgoing longwave radiation. Mon Weather Rev 14:1354–1367

Lau NC, Nath MJ (2009) A model investigation of the role of air–sea interaction in the climatological evolution and ENSO-related variability of the summer monsoon over the South China Sea and Western North Pacific. J Clim 22:4771–4792

Lau KM, Yang GJ, Shen SH (1988) Seasonal and intraseasonal climatology of summer monsoon rainfall over East Asia. Mon Weather Rev 116:18–37

Li HM, Dai AG, Zhou TJ et al (2010) Responses of East Asian summer monsoon to historical SST and atmospheric forcing during 1950–2000. Clim Dyn 34:501–514. doi:10.1007/s00382-008-0482-7

Matthews AJ, Kiladis GN (1999) Interactions between ENSO, transient circulation, and tropical convection over the Pacific. J Clim 12:3062–3086

Murakami M (1979) Large-scale aspects of deep convective activity over the GATE area. Mon Weather Rev 107:994–1013

North GR, Bell TL, Cahalan RF et al (1982) Sampling errors in the estimation of empirical orthogonal functions. Mon Wea Rev 110:699–706

Rayner NA, Parker DE, Horton EB et al (2003) Global analyses of sea surface temperature, sea ice, and night marine air temperature since the late nineteenth century. J Geophys Res. doi:10.1029/2002JD002670

Ren XJ, Zhang YC (2007) Western Pacific jet stream anomalies at 200 hPa in winter associated with oceanic surface heating and transient eddy activity. Acta Meteo Sinica 21:277–289

Seo KH, Schemm J-KE, Wang W et al (2007) The boreal summer intraseasonal oscillation simulated in the NCEP Climate Forecast System: the effect of sea surface temperature. Mon Weather Rev 135:1807–1827

Su B, Gemmer M, Jiang T (2008) Spatial and temporal variation of extreme precipitation over the Yangtze River Basin. Quat Int 186:22–31

Tao SY, Chen LX (1987) A review of recent research on the East Asian summer monsoon in China. Reviews in Monsoon Meteorology. In: Chang C-P and Krishnamurti (eds), Oxford University Press, 60–92

Teng HY, Wang B (2003) Interannual variations of the boreal summer intraseasonal oscillation in the Asian-Pacific region. J Clim 16:3572–3584

Wang B, LinHo (2002) Rainy season of the Asian-Pacific summer monsoon. J Clim 15:386–398

Wang YQ, Zhou L (2005) Observed trends in extreme precipitation events in China during 1961–2001 and the associated changes in large-scale circulation. Geophys Res Lett 32:L09707. doi:10.1029/2005GL022574

Wang B, Wu RG, Fu XH (2000) Pacific-East Asia teleconnection: how does ENSO affect East Asian climate? J Clim 13:1517–1536

Wang YQ, Sen OL, Wang B (2003) A highly resolved regional climate model (IPRC-RegCM) and its simulation of the 1998

severe precipitation event over China. Part I: model description and verification of simulation. J Clim 16:1721–1738

Wang B, Wu ZW, Li JP et al (2008) How to measure the strength of the East Asian summer monsoon. J Clim 21:4449–4463

Wu ZW, He JH, Li JP et al (2006) The summer drought-flood coexistence in the Middle and Lower reaches of the Yangtze River and analysis of its air-sea background feathers in anomalous years (in Chinese). Chin J Atmos Sci 30:570–577

Wu B, Zhou TJ, Li T (2009) Seasonally evolving dominant interannual variability modes of East Asian climate. J Clim 22:2992–3005

Wu B, Li T, Zhou TJ (2010) Relative contributions of the Indian Ocean and local SST anomalies to the maintenance of the western North Pacific anomalous anticyclone during El Nino decaying summer. J Clim 23:2974–2986

Xu Q, Zhang YX (2007) The Meiyu of Huaihe river in recent 52 years (in Chinese). J Appl Meteorol 18:147–157

Xu Y, Xu HC, Gao XJ et al (2009) Projected changes in temperature and precipitation extremes over the River Basin of China in the 21st century. Quat Int 208:44–52

Yang QM (2009) The 20–30-day oscillation of the global circulation and heavy precipitation over the lower reaches of the Yangtze River valley. Sci China Ser D Earth Sci 52:1485–1501

Yang H, Li CY (2003) The relation between atmospheric intraseasonal oscillation and summer severe flood and drought in the Changjiang–Huaihe river basin. Adv Atmos Sci 20:540–553

Yu RC, Zhou TJ (2007) Seasonality and three-dimensional structure of the interdecadal change in East Asian monsoon. J Clim 20:5344–5355

Yu RC, Wang B, Zhou TJ (2004) Tropospheric cooling and summer monsoon weakening trend over East Asia. Geophys Res Lett 31: L22212. doi:10.1029/2004GL021270

Zhai PM, Zhang XB, Wan H et al (2005) Trends in total precipitation and frequency of daily precipitation extremes over China. J Clim 18:1096–1108

Zhang LJ, Qian YF (2003) Annual distribution features of precipitation in China and their interannual variations. Acta Meteor Sinica 17:146–163

Zhang LJ, Qian YF (2004) A study on the feature of precipitation concentration and its relation to flood-producing in the Yangtze River Valley of China (in Chinese). Chin J Geophys 47:622–630

Zhang Q, Chong YX, Jiang T et al (2007) Possible influence of ENSO on annual maximum streamflow of the Yangtze River. China J Hydrol 333:265–274

Zhou TJ, Gang DY, Li J et al (2009a) Detecting and understanding the multi-decadal variability of the East Asian Summer Monsoon—recent progress and state of affairs. Meteorol Z 18(4):455–467

Zhou TJ, Yu RC, Zhang J et al (2009b) Why the Western Pacific subtropical high has extended westward since the late 1970s. J Clim 22:2199–2215

Zhou XX, Ding YH, Wang PX (2010) Moisture transport in the Asian summer monsoon region and its relationship with summer precipitation in China. Acta Meteor Sinica 24:31–42

Zhu XY, He JH, Wu ZW (2007) Meridional seesaw-like distribution of the Meiyu rainfall over the Changjiang–Huaihe River Valley and characteristics in the anomalous climate years. Chinese Sci Bull 52:2420–2428

Zhu J, Huang DQ, Qian YF et al (2010) Uneven characteristics of warm extremes during Meiyu period over Yangtze–Huaihe region and its configuration with circulation systems. Chin J Geophys (in Chinese) 53:2310–2320